ELSEVIER

International Journal of Heat and Fluid Flow 21 (2000) 22–36

International Journal of HEAT AND FLUID FLOW

www.elsevier.com/locate/ijhff

Simultaneous measurements of temperature and velocity fluctuations in a slightly heated jet combining a cold wire and Laser Doppler Anemometry

Laurence Pietri [a], Muriel Amielh [b,*], Fabien Anselmet [b]

[a] *Laboratoire de Mécanique, Acoustique et Instrumentation, 52 Avenue de Villeneuve, 66680 Perpignan Cedex, France*

[b] *Institut de Recherche sur les Phénomènes Hors Equilibre, Université de Marseille, 12 Avenue de Général Leclerc, 13003 Marseille, France*

Received 14 February 1999; accepted 5 October 1999

Abstract

Simultaneous measurements of two velocity components and temperature are performed combining Laser Doppler Anemometry (LDA) and cold wire thermometry. LDA is a common technique suitable for velocity measurements in turbulent jets where strong turbulence intensities and reverse flows may exist, but temperature measurements in association with LDA are difficult because the fine wire response is altered by the seeding deposit, so that the wire must be regularly cleaned. Results reported herein concern velocity–temperature correlations, as well as velocity and temperature marginal probability density functions and temperature (or velocity) probability density functions conditioned by the sign of the velocity (or temperature) fluctuation. The evolution of these various quantities is analysed in order to better understand the mixing properties in the near-field of a turbulent jet where the initial conditions still have a strong influence. It is shown that, while the velocity field tends to relax rather quickly (within a few nozzle diameters from the exit) to almost gaussian statistics, the temperature properties are still significantly skewed towards the hot jet exit temperature until x/D_j about 7–8. On the contrary, the signature of the cold ambient temperature vanishes rather quickly.

Keywords: Slightly heated turbulent jet; Laser Doppler Anemometry; Turbulent heat flux; Temperature probability density function; Scalar mixing

Notation

d	cold wire diameter (m)
d'	spacing between the probe volume and the cold wire (m)
D_j	internal nozzle diameter (m)
F	flatness factor
$F(n)$	contribution to the normalised power spectrum at the frequency n (s)
l	cold wire length (m)
L	half-radius (m)
M	momentum flux (N)
Pr_t	turbulent Prandtl number
r	radial position (m)
Re	Reynolds number
$R_{u\theta}$	correlation coefficient between u and θ
$R_{v\theta}$	correlation coefficient between v and θ
S	skewness factor
$\langle T\rangle$, θ	temperature, mean and fluctuation (K)
$\langle U\rangle$, u	longitudinal velocity component, mean and fluctuation (m/s)
$\langle V\rangle$, v	radial velocity component, mean and fluctuation (m/s)
x	axial position (m)

Greek

α_t	eddy diffusivity (m^2/s)
α_1	temperature coefficient (K^{-1})
η	Kolmogorov length scale (m)
ρ	density (kg/m^3)
γ	intermittency factor
ν_t	eddy viscosity (m^2/s)
ΔT	$\langle T\rangle - T_e$ (K)
ΔU	$\langle U\rangle - U_e$ (m/s)

Subscripts

$(\,)_c$	related to the axis
$(\,)_e$	related to the external flow (or coflow)
$(\,)_j$	related to the nozzle exit
$(\,)_{u \text{ or } v}$	related to one velocity component
$(\,)_\theta$	related to temperature
$\langle\,\rangle$	mean operator

* Corresponding author.
E-mail address: amielh@marius.univ-mrs.fr (M. Amielh).

0142-727X/00/$ - see front matter
PII: S0142-727X(99)00071-5

Superscripts

$*j$	non-dimensionalised by $\Delta U_j\ \Delta T_j$
$*c$	non-dimensionalised by $\Delta U_c\ \Delta T_c$

Abbreviations

p.d.f.	probability density function
r.m.s.	root mean square

1. Introduction

Studying a heated flow where temperature acts as a passive contaminant is a first approach of the problems encountered in air-gas mixing when the gas is present in a low proportion (only a few percents). The next step in studying gas mixing would be the consideration of the scalar mass fraction behaviour which may become active when the pure gas jet develops in ambient air.

The coupling between the velocity and temperature fields in a slightly heated jet is the main object of the present paper. The analysis of these two quantities interaction is essential to understand the transfer mechanisms during the mixing process which occurs within the 20 first diameters of the jet development where very scarce results are available. Moreover, experimental results concerning heat turbulent flux are needed for modelling purposes in numerical applications. In particular, approximating turbulent diffusion by an eddy diffusivity assumption, where the flux is assumed to be proportional to the mean temperature gradient, is often used for modelling applied to industrial problems.

The literature includes a large number of results concerning heated air jets. The recent most important works about heated jets are those by Antonia et al. (1975), Venkataramani et al. (1975), Antonia and Bilger (1976), Chevray and Tutu (1978) and Browne et al. (1984). More recently, a detailed study was performed by Chua (1989) (see also Chua and Antonia, 1990) to investigate the influence of the initial conditions, but also of the wire probe configuration, on various properties associated with second-order moments. The most recent investigations (Antonia and Mi, 1993; Anselmet et al., 1994) deal particularly with the dissipation (or destruction) of temperature fluctuations. Some recent works also concern the study of the scalar concentration and consequently the influence of density variations on the jet development (Pitts, 1991; So et al., 1991; Panchapakesan and Lumley, 1993; Sautet and Stepowski, 1995).

Simultaneous measurements of velocity and temperature are usually performed with multi hot-wire probes. However, it is now recognised that either the flying hot-wire technique or LDA should be used in turbulent jet studies. The idea of using a LDA system and a wire probe is not new. Indeed, Heitor et al. (1985) combined a LDA system and a thermocouple for simultaneous measurements of velocity and temperature in a premixed flame. A similar arrangement was used later on by Neveu et al. (1994). Zhu et al. (1988) developed a technique for measuring turbulent mass fluxes by replacing the thermocouple by a hot wire incorporated inside an aspirating probe which is only sensitive to concentration variations. This technique was also used by So et al. (1991) in a mixed jet of air and helium. This device was modified by Thole and Bogard (1994) for the investigation of a heated boundary layer. In that study, temperature was measured with a 0.63 μm diameter cold wire with the advantage of a good frequency response.

The presently selected method for simultaneous measurements of velocity and temperature is a combination between an LDA system and a cold wire probe. These measurements are performed in a vertical axisymmetric jet set-up. Our results are classified in two ways. First, the various cross moments between the two velocity components, longitudinal u and radial v, and temperature are calculated up to the second order only. Higher order mixed-moments ($\geqslant 3$) were not converged for the largest number of available acquired data (8000 points) and they are not presented here. Consequently, the estimation of the temperature dissipation rate is not possible using the equation for the budget of the temperature variance, because the $\langle v\theta^2\rangle$ term remains unknown. However, the second part of our paper is concerned with probability density functions (p.d.f.s) of the two velocity components and temperature. Indeed, the temperature p.d.f. is a good tool to analyse the statistical properties of the scalar field in turbulent flames or turbulent reactive flows and to assess the main features of the way the scalar is mixed by the turbulent flow field.

2. Experimental set-up

2.1. Slightly heated jet

The experimental study is performed in a vertical jet. Due to its dimensions and characteristics, this facility allows the investigation of the jet turbulence properties from the small to the large turbulent scales. Only a brief description is given here, details can be found in Bonnelye (1991) and Djeridane (1994).

The experimental set-up is a fully developed turbulent pipe jet, axisymmetric, ascending, without rotation, exhausting in a low speed turbulent air coflow. The inside diameter of the jet nozzle is $D_j = 26$ mm and its thickness 0.8 mm (Scheme 1).

The presence of the air coflow is very useful to control the boundary conditions for further comparison with turbulence modelling results. The flow is slightly confined in a square cross-section enclosure (285×285 mm^2) so that the cross-section ratio between the enclosure and the nozzle is greater than 100. Seeding both flows (jet and coflow) reduces the difficulties associated with LDA measurements in the jet off-axis region (Djeridane, 1994). The coflow velocity is small enough to avoid any strong influence on the jet development and large enough to obviate any reverse flows. This latter feature is insured here because the Craya–Curtet number is greater than 0.8

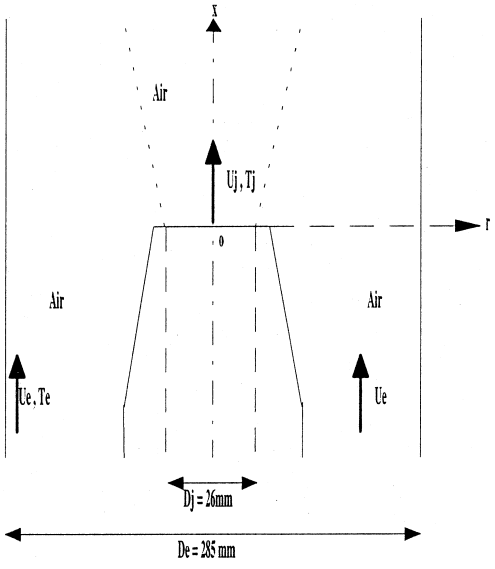

Scheme 1. Experimental set-up.

(Bonnelye, 1991). The overall height of the facility is 12 m, but the part available for experiments is only 1.5 m ($\approx 40D_j$) high.

In order to mark the flow and then approach the concentration field of a variable density jet with low density gradients, the primary jet may be heated

$$\Delta T_j = T_j - T_e = 20 \text{ K} \quad \Rightarrow \quad \rho_j/\rho_e = 0.94,$$

so that temperature then acts as a passive contaminant with respect to the velocity field.

In their near-field, jet flows are strongly dependent on the exit Reynolds number Re_j. This dependence is reduced when the Reynolds number becomes very large. Pitts (1991) showed that the Reynolds number effects are small for Reynolds numbers larger than 50 000. In the present study, the Reynolds number ($Re_j = 21\,000$) is large enough to insure a fully turbulent ejecting jet. The exit velocity is $U_j = 12$ m/s on the axis. The velocity of the air coflow is 0.9 m/s.

The nominal momentum flux ($= (\pi/4)D_j^2\rho_j U_j^2$) is $M_j = 0.1$ N ($M_j/M_e \approx 1.16$). Knowing this parameter is essential for further comparison with results obtained in variable density jets (helium or CO_2 jets). Indeed, momentum whose dimension is that of a force is a more physical parameter than the Reynolds number for such a comparison. With the same M_j, the ejection regions of different gas jets are subject to the same force. For a given density and a given exit diameter, M_j is controlled by the exit velocity.

Various measurements of velocity and temperature were performed on the jet axis and in many radial sections. In each section, only half-profiles were considered because of the axisymmetry of the flow.

2.2. Laser Doppler Anemometry

Velocity measurements are performed with a Laser Doppler system using the 488 and 514.5 nm wavelengths of a Spectra Physics 4 W argon laser source. The light is transmitted from the source to the emission-reception head by 10 m long optical fibres, and backscatter detection is used. Four beams are emitted, two blue and two green. A Bragg cell is used. The probe measuring volume ($0.09 \times 0.09 \times 0.8$ mm^3) is located at a 310 mm focal distance from the head. The fringe planes are inclined with a 45° angle to the jet axis in order to obtain an equivalent sensitivity on both velocity signals. Then instantaneous $U+V$ and $U-V$ data are measured. The reliability of the V radial component measurements was checked by comparing the mean values $\langle V \rangle$ with those deduced from $\langle U \rangle$ measurements and the continuity equation. On the axis, in the section $x/D_j = 15$, where $\langle V \rangle$ should be zero, Djeridane et al. (1996) measured $\langle V \rangle$ equal to 0.3% of the longitudinal mean velocity $\langle U \rangle$.

Both flows (primary jet and coflow) are seeded by silicone oil droplets (silicone 710, 1.11 density, 500 mm^2/s kinematic viscosity). The diameter of the droplets is about 1 μm. The aerosol is generated by perfume diffusers (SIBE) using compressed air.

The importance of getting measurements in the jet outer region for mixing studies explains the present interest in the coflow seeding. The good agreement between measurements of $\langle V \rangle$ and calculations using the continuity equation was a first verification of the good seeding on the jet edges. Another check was provided by Gharbi et al.'s (1995) study which investigated the interface region of variable density jets in the same facility. These authors showed a very good agreement of the velocity variances in the jet edges with a r^{-4} power law as predicted by Phillips' theory.

The velocity signals are acquired by two Burst Spectrum Analysers (BSA 57N10, DANTEC). Data are transferred onto an HP Vectra XM 5/90 Personal Computer where they are processed in order to obtain the U and V velocity components and their various moments.

2.3. Cold wire thermometry

Cold wire thermometry is a fine technique to measure temperature fluctuations. Many considerations must be taken into account to optimise such measurements.

A 0.63 μm diameter wire is chosen in order to minimise the thermal inertia and to get access to the highest frequency fluctuations of the flow temperature. The time constant, which depends directly on the wire diameter d, must be as small as possible (Fulachier, 1978). The cut-off frequency related to the time constant is 10 kHz for the (maximal) exit velocity and 5 kHz for the (minimal) velocity on the jet edge.

End effects due to the heat loss through the prongs and to the development of thermal boundary layers around the prongs affect the temperature variance measurements (Paranthoen et al., 1982). These effects are reduced when choosing a wire with a suitable sensitive length l or more precisely with a suitable ratio l/d. A ratio greater than 700 is usually recommended (Antonia and Mi, 1993). Moreover, when the silver jacket of the Wollaston wire is left on both ends of the sensitive part, the response of the probe is improved because the sensitive part is outside the thermal boundary layers. However, the etched length must not be too long to avoid the problem of spatial integration. Wyngaard (1971) showed that, for l/η inferior to 3, where η is the Kolmogorov length scale, the effect of spatial integration is negligible. Nevertheless, Ould-Rouis (1995) showed that a l/η ratio of 6 is still satisfactory. An acceptable compromise for the wire length must be found in order to minimise the end effects without deterioration of the spatial resolution.

The chosen wire is herein a Wollaston wire with a Platinum – 10% Rhodium core and a silver jacket (≈50 μm diameter). Its total length is 4 mm and the sensitive etched length is 0.5 mm. With a 0.63 μm diameter wire, the l/d ratio is then about 800 and the l/η ratio varies in the range 3–13 along the axis. In particular, measurements in the section $x/D_j = 5$ ($l/\eta = 13$) are performed with a very bad resolution of the small scales. Nevertheless, studying the turbulent fine structures is not the objective of the present work.

Most of the measurements were made with a 0.63 μm diameter wire, but a 1.2 μm diameter wire was also used for some of them. The temperature coefficients of these wires are respectively 1.65×10^{-3} K^{-1} and 1.4×10^{-3} K^{-1}.

The cold wire is operated with a constant current (0.2 mA) anemometer. The whole thermometry system consists in the assembly of three modules:

- a Wheatstone bridge which includes the cold wire in one of its branches, associated with a pre-amplification stage with a tuning gain;
- a second amplification stage with a tuning gain and an offset;
- a low-pass filter.

Data are acquired with an A/D (12 bits) Lab-PC card (National Instruments). The maximum available sampling frequency is 62.5 kHz.

2.4. Optimising simultaneous measurements of velocity and temperature

In order to measure simultaneously two velocity components and temperature, an acquisition of the temperature signal by the Lab-PC card is triggered by the detection of a burst by the BSAs. An electronic system of synchronisation, built in our institute (Pietri et al., 1997), plays the role of an interface

between the BSAs (velocity) and the Lab-PC card (temperature). This synchronisation system ensures, firstly, a simultaneous start for the card and the BSA's acquisitions and, secondly, the coupling of a burst (velocity) to a cold wire data point (temperature) without ambiguity. The time delay between the measurements of velocity and temperature, imposed by the electronic system, is estimated to be about 2 μs. In the best case, one burst corresponds with one temperature sample. However, some bursts, too close from the previous one in time ($1/\Delta t > 62.5$ kHz), do not have any temperature image. Some triplets (U, V, θ) are also eliminated by a home-made processing software because the velocity detection is invalid.

A specific problem resulting from the present technique is the deposit of oil droplets on the cold wire due to seeding. Then, the effective diameter of the wire increases and its response is progressively modified because its thermal inertia is increased. Fig. 1 presents the temperature power spectrum in the frequency domain $F(n)$, with $\int_0^\infty F(n)\,dn = 1$. Indeed, the temperature power spectrum is clearly affected for frequencies larger than 200 Hz when the wire is dirty after a long exposure to the seeding droplets. However, if the data acquisition time does not exceed 90 s at $x/D_j = 5$ and 350 s at $x/D_j = 15$ on the axis, it is possible to clean the wire and to restore its frequency response (Hilaire, 1992). The cleaning method consists either in dipping the wire in an acetone bath crossed by ultrasonic waves or in burning the deposited oil by increasing the overheat current of the wire. The second solution is easier to implement.

The wire is positioned close to the laser probe volume using micrometric manipulators in the three main directions. The spatial resolution of the displacement is 0.01 mm along the lateral direction perpendicular to the laser head axis – direction of V measurements – and 0.02 mm along both other directions (along the vertical axis = jet axis and along the head axis). The value of the angle between the wire and the main direction of the laser probe volume was shown to have no effect on the velocity–temperature correlation coefficient $R_{u\theta}$.

The optimal spacing d' between the probe volume and the wire is searched with a two beam laser configuration (measurement of only one component). The minimum value of d' is 2η at $x/D_j = 0.2$. By comparison with the reference value of $R_{u\theta}$ obtained by Chevray and Tutu (1978), at $x/D_j = 15$ on the axis of a slightly heated jet, our correlation is best measured when d' is in the range 2.5–4η. During the measurement of two velocity components, the configuration remains optimal since the minimum spacing we can achieve with the four laser beams is 3.5η.

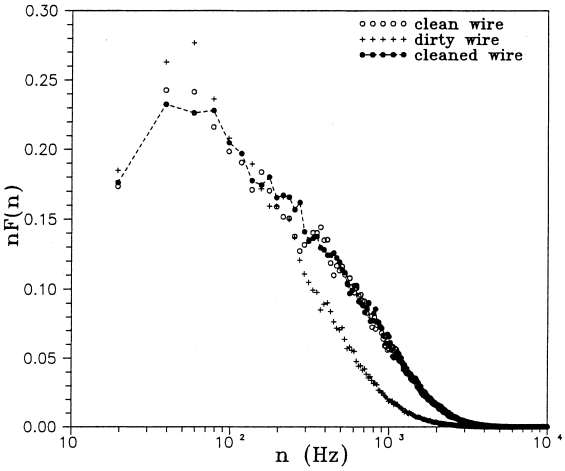

Fig. 1. Temperature spectrum: before and after the exposure to the seeding; before and after the cleaning of the wire with acetone.

The influence of the wire probe on the velocity measurement was also studied. Between 2.5 and 4η, the error on the mean velocity is around 4%. The error is only 2.5% on the velocity r.m.s. Therefore, the effect of the presence of the wire in the vicinity of the LDA probe volume remains negligible for this range of spacing. For results reported herein, no correction is applied on the LDA velocity measurements. Note that Zhu et al. (1988) did not find any influence of the presence of their concentration probe for a spacing $d' = 4\eta$.

At the opposite, the presence of the LDA probe volume seems to have no influence on the temperature measurements. There is only a strong imbalance of the Wheatstone bridge when the laser beam touches the wire.

3. Cross moments

3.1. Heat turbulent flux and correlation coefficient

On the axis, the measured correlations involving the radial velocity component are almost zero in agreement with the flow symmetry. Therefore, the corresponding data are not presented here.

Fig. 2 presents, both in linear (Fig. 2a) and logarithmic (Fig. 2b) scales, the evolution of the longitudinal turbulent heat flux $\langle u\theta \rangle$ along the jet axis, together with those for the associated correlation coefficient $R_{u\theta}$ and the r.m.s. values u', v' and θ'. All these results are presented using normalisation by the initial mean differences of velocity and/or of temperature. The logarithmic presentation clearly highlights the three different regimes of the jet evolution. In the first diameters, all these quantities have a constant level at the value equal to that typical for a fully turbulent pipe flow, whereas, in the far-field region, all these quantities (except $R_{u\theta}$ which remains constant) display power-law evolutions characteristic of a fully developed turbulent jet flow regime. The most striking feature is the earlier development of the temperature field, since θ' starts increasing from the station x/D_j about 3, whereas u' and v' only start increasing from x/D_j about 5. These positions are very closely associated with those where the skewness factors of θ and u get their minimal values (see also Fig. 6 for the complete discussion of the skewness longitudinal evolutions), these minimal values reflecting the appearance on the jet axis of significant amounts of poorly mixed blobs of ambient fluid.

Therefore, one could define a thermal potential core extending to x/D_j about 3 and a dynamic potential core extending to x/D_j about 5. The origin of the different locations for the end of these "potential cores" is still not very clear, it is probably associated with the slightly different initial conditions for the thermal and dynamic fields, since the pipe wall is almost perfectly insulated from the ambient temperature (which results in an almost uniform temperature and a very small level of $\theta'/\Delta T_j$ within the pipe since the ambient temperature T_e is involved in ΔT_j). On the contrary, the dynamic field is subject to two very different boundary conditions, the zero velocity at the wall and the maximum velocity on the centreline (which results in levels of about 0.04 for both $u'/\Delta U_j$ and $v'/\Delta U_j$ within the pipe). Therefore, the main difference between the velocity and temperature fields results from the fact that the low velocity limit does not change significantly when moving from the pipe to the region of jet development (in fact, $U_e = 0.9$ m/s due to the coflow) whereas the low temperature limit changes abruptly to the ambient temperature T_e (which is significantly lower than the pipe wall temperature). In classical litterature experiments, the temperature condition on the nozzle wall is not specified, but it is probably rather close to

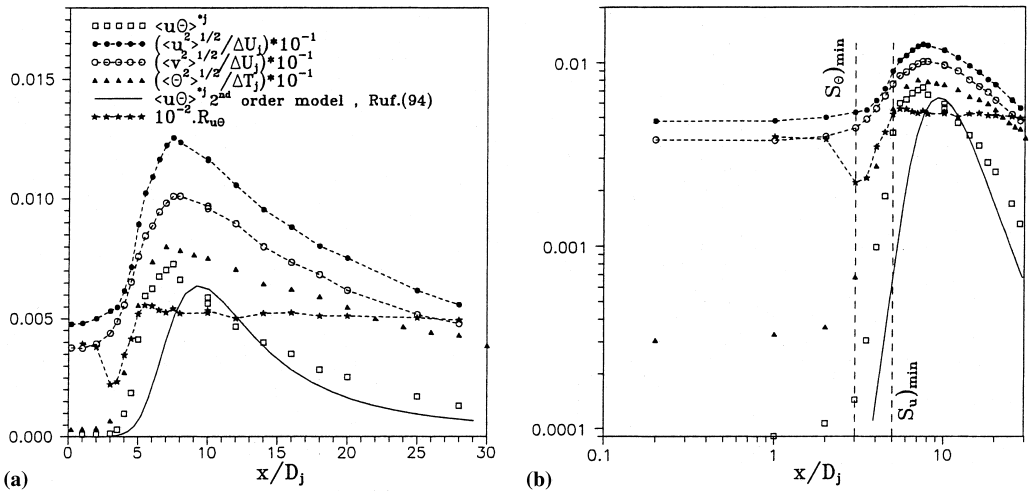

Fig. 2. Axial evolution of the longitudinal heat flux $\langle u\theta \rangle$ and of the r.m.s of the longitudinal and radial velocity components and of temperature. (a) Linear scales; (b) logarithmic scales.

the ambient one since the near-field evolutions of u' and θ' are generally very similar (e.g. Browne et al., 1984). However, in most of the "non-academic" situations (including, of course, industrial situations), the temperature wall condition is likely to change from one case to another, and to be quite unprecisely defined too, and it is therefore important to note that the temperature and velocity near-field evolutions may be significantly different (as in the present case).

The evolution of the flux $\langle u\theta \rangle$ is rather similar to that of θ' in the near-field region, also starting from a very small value, while it finishes with a -2 exponent power law in the far-field region. The experimental data are in general good agreement with the numerical data obtained by Ruffin (1994) using a second-order model, except for a slight shift of the position of the $\langle u\theta \rangle$ maximum (which is probably associated with slightly different initial conditions since $\theta'/\Delta T_j$ is equal to zero for the exit nozzle numerical data, see Ruffin et al., 1994). However, the associated correlation coefficient $R_{u\theta}$ does not change much, except for a slight decrease over the region $(2 < x/D_j < 6)$ where our temperature field evolution is initiated before that for the velocity field.

3.2. Some sections of the jet

It appears from the previous observations that two sections are of particular interest. The first one is located at the end of the dynamic potential core, $x/D_j = 4.5$. At this station, the axisymmetric mixing layer which develops from the nozzle reaches the jet axis so that the velocity skewness and flatness factors then get their extremal values. The behaviour of the heat turbulent fluxes is here interesting to study. The second section to be more thoroughly investigated in the present work is $x/D_j = 15$ where the jet is close to be fully developed in terms of the second-order moments of velocity and of temperature (as seen in Fig. 2b).

Fig. 3 presents the radial evolution of the longitudinal $\langle u\theta \rangle$ and radial $\langle v\theta \rangle$ turbulent fluxes, normalised by the mean differences of velocity and of temperature on the axis, in the sections $x/D_j = 4.5$ and 15, where the radial position is normalised by the half velocity radius. The almost zero value of the flux $\langle v\theta \rangle$ measured on the axis claims the quality of these measurements. The radial position where the fluxes are maximal is the same for these two sections and corresponds to the

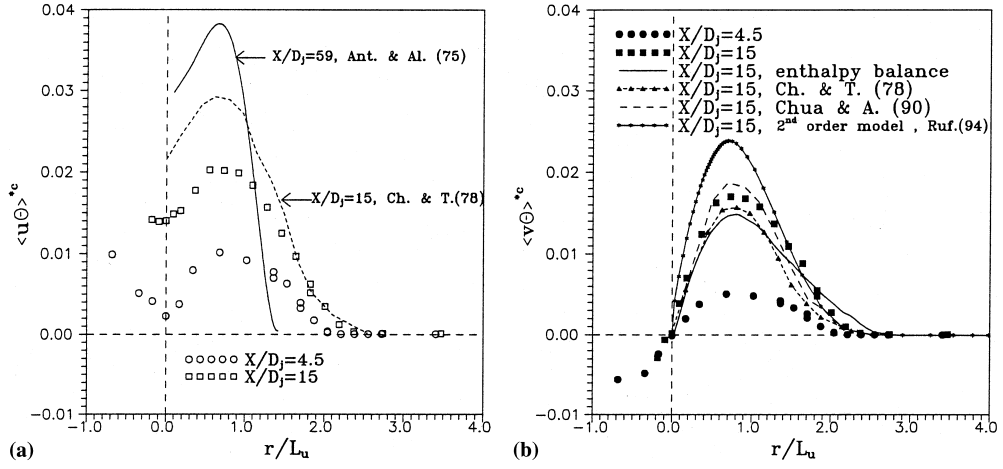

Fig. 3. Radial evolution of (a) longitudinal and (b) radial heat fluxes in two sections of the jet.

position where the turbulent kinetic energy is maximal. It agrees reasonably well with the position given by Chua and Antonia (1990), $r/L_u = 0.7$, and by Chevray and Tutu (1978), $r/L_u = 0.8$.

However, when these profiles are compared in more detail, the results we presently obtain at $x/D_j = 15$ differ quite significantly, especially for the longitudinal heat flux, from those found in the literature like in the works by Antonia et al. (1975), at $x/D_j = 59$, or by Chevray and Tutu (1978), at $x/D_j = 15$, both in terms of raw non-normalised data and of dimensionless normalised data. This latter point, which is closely connected to the jet expansion, depends on the presence and the strength of the coflow. The $\langle u\theta\rangle$ profile has a wider extent when the coflow velocity U_e is decreased: Chua and Antonia and Chevray and Tutu study the free jet case, whereas Antonia et al. (1980) present a case with a strong coflow ($U_j/U_e = 6.6$). Note the value of $U_j/U_e = 13$ in the present work. The presently obtained $\langle u\theta\rangle$ values are lower than those of the literature. The reason is probably related to the emission conditions of the jets, laminar for the previously quoted studies and fully turbulent for our experiments, which influence the development of the various turbulent quantities in jets. The effect of the initial conditions on the dynamic field was studied in the past by Hussain and Zedan (1978) and Russ and Strykowski (1993). A likely explanation is also given by Chua and Antonia who reach very early ($x/D_j = 15$) the self similarity regime in their studied jet. Results obtained for the radial heat flux agree with those of Chua and Antonia (1990) at $x/D_j = 15$. The comparison with the second-order model (Ruffin, 1994) is not so good because the calculated radial heat flux is overestimated.

In Fig. 3, the radial profile of the radial heat flux $\langle v\theta\rangle$, as deduced from the enthalpy equation (1), is also presented

$$\langle U\rangle\frac{\partial\langle T\rangle}{\partial x} + \langle V\rangle\frac{\partial\langle T\rangle}{\partial r} + \frac{\partial\langle u\theta\rangle}{\partial x} + \frac{1}{r}\frac{\partial\langle rv\theta\rangle}{\partial r} = 0, \tag{1}$$

$$\langle v\theta\rangle = \frac{1}{r}\int_0^r r\left[\langle U\rangle\frac{\partial\langle T\rangle}{\partial x} + \langle V\rangle\frac{\partial\langle T\rangle}{\partial r} + \frac{\partial\langle u\theta\rangle}{\partial x}\right]\mathrm{d}r.$$

This calculation under-estimates the $\langle v\theta\rangle$ flux as compared to the measurements. This discrepancy, observed for radial positions larger than $r/L_u = 0.4$, is due to the fact that the derivative of $\langle u\theta\rangle$ was neglected in our calculation using (1). Indeed, Djeridane (1994) showed that the $\langle v\theta\rangle$ value is increased if the axial gradient of $\langle u\theta\rangle$ – which was then provided by the second-order model of Ruffin (1994) – is taken into account. As the flux measurements were realised in only a few sections, it was not possible to calculate the axial $\langle u\theta\rangle$ gradient with the present experimental data, except on the axis.

Some estimations of the measurement errors can be deduced from the calculation of the different terms of Eq. (1) on the axis. Table 1 gives these different terms calculated for the sections $x/D_j = 4.5$ and 15. The second term of (1) is zero because $\langle V\rangle$ and the radial gradient of $\langle T\rangle$ are zero on the axis. The three other terms are assumed to be related to the first one.

Table 1
Magnitude order of the different terms of (1) calculated on the jet axis

Terms in Eq. (1)	$x/D_j = 4.5$	$x/D_j = 15$
$\langle U\rangle\frac{\partial\langle T\rangle}{\partial x}$	1	1
$\frac{\partial\langle u\theta\rangle}{\partial x}$	−0.076	0.005
$\frac{1}{r}\frac{\partial}{\partial r}(r\langle v\theta\rangle) = 2a$	−1.001	−0.891

As a first approximation, one can write that the $\langle v\theta\rangle$ flux varies linearly with r around $r = 0$, so that $\langle v\theta\rangle = ar$. The third term is then equal to $2a$. The sum of these three quantities should be zero. The cause of this imbalance is probably a bad estimation of the gradients, but particularly of the coefficient a, because the symmetry of $\langle v\theta\rangle$ around $r = 0$ is not perfectly satisfied by our measurements.

In the very near field ($x/D_j = 4.5$), the heat flux is preferably active along the longitudinal velocity: $\langle u\theta\rangle/\langle v\theta\rangle = 2$ between $r/L_u = 0.2$ and 1.4. Downstream ($x/D_j = 15$), the contributions tend to be equivalent: $\langle u\theta\rangle/\langle v\theta\rangle$ is around 1.1 between $r/L_u = 0.5$ and 1.8. This ratio is also found rather constant, slightly inferior to 2, in a turbulent plane jet ($Re_j = 7900$, $\Delta T_j = 25$ K) by Antonia (1985) at $x/D_j = 40$, between $r/L_u = 0.4$ and 1.3. In an axisymmetric jet with a strong coflow ($U_j/U_e = 6.6$), far downstream at $x/D_j = 59$, Antonia et al. (1975) measure longitudinal and radial heat fluxes with a ratio of 1 between $r/L_u = 0.3$ and 1.3.

3.3. Correlations and interface positions

The radial profiles of the correlation coefficients $R_{u\theta}$ and $R_{v\theta}$ are presented for the same sections as before ($x/D_j = 4.5$ and 15) in Fig. 4. The correlation coefficients R_{uv} between the longitudinal and radial velocity components are also plotted on these graphs.

At $x/D_j = 4.5$, the longitudinal correlation coefficient $R_{u\theta}$ is rather constant between $r/L_u = 0$ and 1.7. It slightly varies around the value 0.5. It then decreases to 0.15 at $r/L_u = 2.2$. Beyond $r/L_u = 2.5$, $R_{u\theta}$ seems to tend to a plateau value in the range 0.4–0.5, but such measurements on the jet edge are very difficult, so that the associated errors may be large. The radial correlation coefficient $R_{v\theta}$ shows a behaviour similar to $R_{u\theta}$ for $r/L_u > 0.3$, with a constant level around 0.38 between $r/L_u = 0.3$ and 1.7. Close to $r/L_u = 0$, the gradient of $R_{v\theta}$ is very high. The correlation coefficient R_{uv} is larger: it reaches a level of 0.45, but its behaviour is very similar to that of $R_{v\theta}$.

At $x/D_j = 15$ (Fig. 4b), the profiles for all correlation coefficients are smoother. $R_{u\theta}$ is constant and equal to 0.52 up to $r/L_u = 1.7$, but reaches a slight minimum of 0.5 on the axis. This result is comparable to that of Chevray and Tutu (1978) who obtain $R_{u\theta} = 0.5$ in the same section, between $r/L_u = 0$ and 1.8. Beyond $r/L_u = 1.7$, $R_{u\theta}$ decreases to a value of 0.36 around the position $r/L_u = 2.3$. It then increases again to a value of about 0.45. The correlation coefficient $R_{v\theta}$ reaches a maximal value of 0.46 on a smaller range of radial positions. Such a plateau is also obtained by Chua and Antonia (1990), despite the stronger ($\theta'_c/\Delta T_c = 0.25$) level of the temperature turbulent intensity than in the present case ($\theta'_c/\Delta T_c = 0.14$). The $R_{v\theta}$ gradient around the axis at $x/D_j = 15$ is twice lower than that at $x/D_j = 4.5$. The R_{uv} behaviour is similar to that of $R_{v\theta}$. The ratio $R_{uv}/R_{v\theta}$ is close to 1 although it was 1.2 at $x/D_j = 4.5$: the turbulent motions seem to be as efficient for the momentum transfer as for the heat transfer at $x/D_j = 15$. This conclusion is opposed to the results of Chevray and Tutu who obtain $R_{uv}/R_{v\theta} = 0.8$.

The minima of the radial profiles of the three correlation coefficients are reached for radii close to those corresponding to the minimum of the intermittency factor γ (Figs. 4(a) and (b)), with γ approached by the relation $\gamma = 3/F_u$ based on the assumptions of a normally distributed turbulence and of a hit-or-miss phenomenon (e.g. Klebanoff, 1954). For R_{uv}, this finding is clearly verified. However, the position of the minimum of $R_{u\theta}$ or $R_{v\theta}$ corresponds better with the minimum of the thermal intermittency factor defined using the flatness factor of temperature, $\gamma_\theta = 3/F_\theta$. The position of the minimum of $R_{u\theta}$ is therefore related to the jet interface location, characterised by an intermittency factor lower than 0.5 (Gharbi et al., 1995).

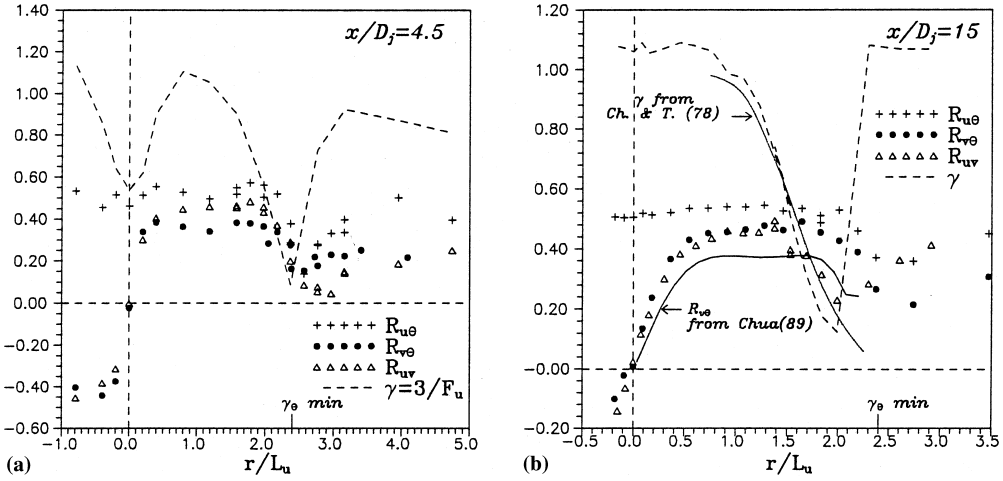

Fig. 4. Radial evolution of the correlation coefficient and the intermittency factor, (a) at $x/D_j = 4.5$; and (b) at $x/D_j = 15$.

Note that qualitatively similar results are obtained in the near-field region, and even on the axis, where $R_{u\theta}$ was shown to attain a minimum value for x/D_j between 2 and 4, this minimum value being associated with the strongly intermittent engulfment of almost unmixed ambient fluid as will be discussed in more detail in the p.d.f. analysis reported in Section 4.

This connection between minimum values in the axial and radial distributions of $R_{u\theta}$, $R_{v\theta}$ and R_{uv}, and the position of an intermittent interface of the jet results from intricate properties of the turbulent mixing process, which obviously need further investigations. In fact, as briefly discussed by Lucas et al. (1998), in these intermittent regions, it appears that conditional averages of either u ($\langle u/\theta_0 \rangle$) or v ($\langle v/\theta_0 \rangle$), for the different temperature fluctuations θ_0, are separated in two different classes. Both classes present classical linear evolutions for these conditional averages, but one class, for the temperature fluctuations which correspond to "well-mixed turbulent fluid", gives linear evolutions of $\langle u/\theta_0 \rangle$ or $\langle v/\theta_0 \rangle$ associated with a slope of about 0.5–0.6, whereas the other class, for the temperature fluctuations very close to the limit T_e (or T_j), also presents a linear evolution but with a much lower slope. The "global" correlation coefficient is then a combination of these two slopes, and it is significantly smaller than the value characteristic of the "well-mixed turbulent fluid". This means that velocity fluctuations associated with the temperature range close to the limit T_e (or T_j) are restricted to a domain of reduced extent. In particular, for $R_{v\theta}$, both at $x/D_j = 4.5$ and $x/D_j = 15$, a small negative (and almost constant) value of $\langle v/\theta_0 \rangle$ is obtained (not shown here) over the interface region for the temperature fluctuations which cover the range between T_e and $T_e + 1.5\theta'$ to $2\theta'$. This explains why $R_{v\theta}$ is more reduced than $R_{u\theta}$ over the intermittent region since this range of temperature fluctuations will have an almost zero contribution to the "global" $R_{v\theta}$ value.

3.4. Turbulent Prandtl number estimation

Using the measurements of the fluxes $\langle v\theta \rangle$ and the radial profiles of the mean temperature, the eddy diffusivity may be estimated when the assumption of diffusion by the mean gradient is made:

$$\alpha_t = -\frac{\langle v\theta \rangle}{(\partial \langle T \rangle / \partial r)}.$$

On the axis, where these two quantities are zero, the eddy diffusivity is estimated using two approximations. The first one concerns the behaviour of $\langle v\theta \rangle$ around $r = 0$: $\langle v\theta \rangle = ar$. The second one is the parabolic law followed by the radial profile of temperature around $r = 0 : \langle T \rangle = a'r^2 + b$. The axial value of the eddy diffusivity is then approached by: $-a/2a'$.

Fig. 5a presents the radial evolutions of the eddy diffusivity and the eddy viscosity at $x/D_j = 4.5$ and 15 (details on the calculation of v_t are given in Djeridane et al., 1996) calculated using measurements of velocity and temperature. The eddy viscosity has a similar behaviour in the two studied sections to that obtained by Djeridane et al. (1996) using a slightly different LDA arrangement. The eddy diffusivity α_t is rather constant (0.008) over the major part of the section $x/D_j = 4.5$, up to $r/L_u = 2$. More downstream in the jet, at $x/D_j = 15$, v_t and α_t evolve similarly. The maximal value of α_t, normalised by the mean difference of velocity and the half velocity radius, obtained at the radius $r/L_u = 0.5$, is about 0.032, which is very close to the value of 0.033 found by Chua and Antonia (1990) at the same section. Chua and Antonia observe in this section a constant value of α_t between $r/L_u = 0.5$ and 1. Their estimated eddy viscosity depends on the cross wire probe they use: for a 90° angle, they propose $v_t = 0.02(\Delta U_c L_u)$ and for a 120° angle, $v_t = 0.025(\Delta U_c L_u)$, this latter value being in agreement with the calculation deduced from the similarity assumptions in jets.

For more downstream sections, the relative behaviour of v_t and α_t is inverted, α_t becoming greater than v_t at $x/D_j = 15$. At $x/D_j = 8$, these two quantities are almost equal (not shown here, v_t and α_t were obtained for this section at radial positions between $r/L_u = 1$ and 3). A good parameter to study this relative behaviour is the turbulent Prandtl number: $Pr_t = v_t/\alpha_t$ (Fig. 5b). It is usually admitted that Pr_t is around 0.7 in free flows such as jets and 0.9 in wall flows. Chambers et al. (1985) note a Pr_t variation in the range 0.4–0.8 in turbulent plane and axisymmetric jets and in wakes.

In the section $x/D_j = 4.5$, the variation of Pr_t is very large: it varies from 0.8 to unusual values of 1.75 ($Pr_t > 1$). In this section, where the dynamic mixing layer which develops over the nozzle reaches the axis a few D_j units after the thermal one, such a behaviour is not surprising considering the results reported in Fig. 2. Browne et al. (1984) also found a large variation of Pr_t in the interaction region of a turbulent plane jet, but with a value which remained lower than 1, except in the region very close ($0 < r/L_u < 0.3$) to the axis (the axis values being generally larger than 1.5). Further downstream, the

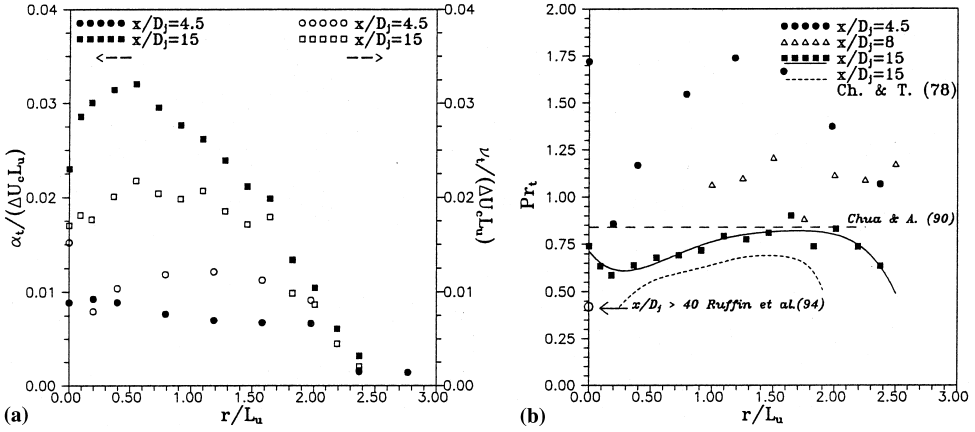

Fig. 5. Radial evolution of (a) eddy diffusivity and (b) turbulent Prandtl number.

turbulent Prandtl number decreases progressively towards the value usually found in jet flows (Antonia and Bilger, 1976; Chevray and Tutu, 1978; Amielh, 1989). At $x/D_j = 15$, Pr_t is around 0.75, except near the axis ($r/L_u < 0.5$). This "plateau" level is in agreement with results of Pr_t obtained by using the similarity shapes of the velocity and temperature radial profiles and the hyperbolic axial decrease of these quantities (Chen and Rodi, 1980). Indeed, with such assumptions-well verified quite far from the exit section-a constant value of Pr_t over the whole section is found, which is directly related to the half-radii by: $Pr_t = (L_u/L_\theta)^2$, so that $Pr_t = 0.72$ is deduced. The turbulent Prandtl number estimated by Chua and Antonia (1990) by measurements with cross wires is about 0.65 (90° angle) or 0.81 (120° angle) for r/L_u between 0.1 and 1. Chevray and Tutu (1978) obtained also $Pr_t = 0.65$ with 90° cross wires. However, the value of 0.81 is probably the right one according to Chua and Antonia, because the 90° cross wires underestimate the flux $\langle uv \rangle$. On the axis, in the far field of the jet ($x/D_j > 40$), Ruffin et al. (1994) propose, with their second-order model, a very low value of $Pr_t = 0.42$ which is not in agreement with most of the experimental data in axisymmetric jets.

This turbulent Prandtl number is an indicator of the difference between the momentum and the heat turbulent transfers. In the near field, at the station $x/D_j = 4.5$, the turbulent motion seems to be more efficient for the transfer of momentum than for heat because $Pr_t > 1$, but this is associated with the strong engulfment of ambient air at this station where the dynamic mixing layer reaches the axis : this high value of Pr_t is probably related to the initial differences between the velocity and temperature fields, so that this feature is likely to change from one jet flow to another.

At $x/D_j = 15$, our Pr_t profile is in reasonable agreement with the (systematically lower) values obtained by Chevray and Tutu (1978), although these ones are deduced from a wrong $R_{uv}/R_{v\theta}$ ratio (see paragraph 3.3), as $\langle uv \rangle$ was then underestimated by measurements (following the argumentation developed by Chua and Antonia, 1990).

4. Probability density functions of temperature and velocity

In order to study in more detail the mixing properties associated with both the temperature and the velocity field, we will present in this section typical p.d.f.s of temperature and velocity. In particular, examining conditional p.d.f.s of temperature, conditioned by the occurrence of either positive or negative longitudinal velocity fluctuations, and conditional p.d.f.s of velocity, conditioned by the occurrence of either positive or negative temperature fluctuations, will allow us to better understand the intricate coupled properties (e.g. Fig. 2) of the temperature and velocity fields in the near-field region.

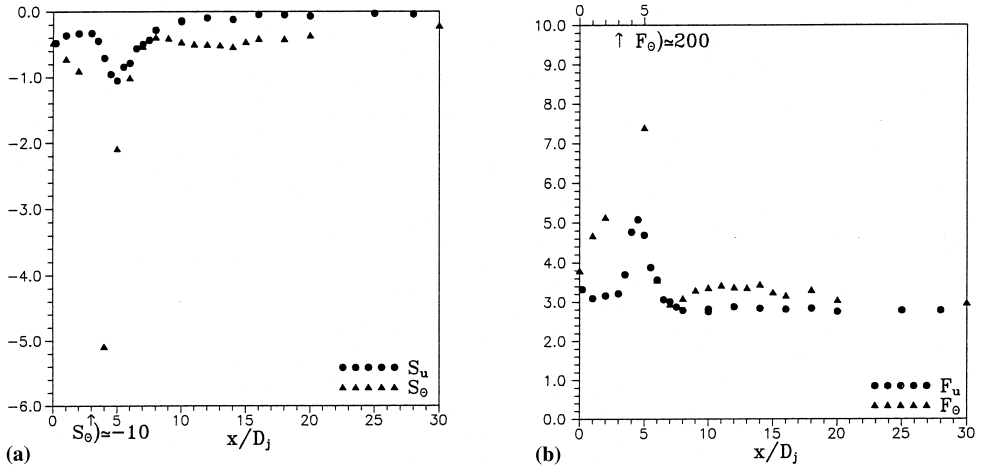

Fig. 6. Axial evolution of (a) skewness and (b) flatness factor of u and θ.

4.1. Skewness and flatness factors of temperature and velocity

The axial evolutions of the skewness (S_θ, S_u, Fig. 6a) and flatness factors (F_θ, F_u, Fig. 6b) of temperature and velocity are presented in Fig. 6. In spite of rather similar values at the nozzle exit (these values being characteristic of fully developed turbulent pipe flow conditions), the near-field ($0.2 < x/D_j < 8$) behaviours of the temperature and velocity fields are rather different: as already observed in Fig. 2, the temperature evolution is much faster than that of velocity. In particular, S_θ and F_θ reach extremal values at x/D_j about 3, whereas S_u and F_u do it at x/D_j about 5. These locations are characteristic of the positions where the thermal and velocity initial mixing layers reach the axis. As explained in Section 3.1, the origin of the different locations for the end of these "potential cores" is still not very clear, it is probably associated with the slightly different initial conditions for the thermal and dynamic fields. It is also interesting to note that the extremal values of S_θ and F_θ are much larger than those of S_u and F_u, indicating the presence of very poorly mixed pockets of fluid at low (i.e. quite close to ambient) temperature. On the contrary, probably because of the combination of the redistribution process associated with pressure and of the limit conditions we have discussed previously, the velocity field does not possess such an intermittent character. However, very similar tendencies can be observed in the temperature S_θ (with $-S_\theta$ becoming as large as 8 at $x/D_j = 4$) and F_θ axial evolutions reported by Browne et al. (1984) in the interaction region of a plane jet, except that the jet temperature field development is only initiated after $x/D_j = 3$. Unfortunately, these authors do not provide any basis for comparing these properties for their temperature and velocity fields.

As a consequence, $R_{u\theta}$ was found (see Fig. 2a) to decrease in the region between $x/D_j = 0.2$ and 3, where cold θ fluctuations appear so that S_θ becomes strongly negative as fluid motions from the primary jet – S_u and F_u do not vary yet (Fig. 6a and b) – tend to be cooled by the ambient coflow. The result is the correlation between a quantity, u, attached to the primary flow, and a quantity, θ, which begins to feel the influence of the secondary flow, and this induces a decrease of $R_{u\theta}$. The minimum of $R_{u\theta}$ ($=0.2$) is reached at the same section ($x/D_j = 3$) where extrema are obtained for S_θ and F_θ. When S_u and F_u begin to change downstream of $x/D_j = 3$, external fluid pockets (low speed, S_u strongly negative) reach the jet axis. There is then more opportunity for u and θ to be representative of the same occurrence. Consequently, $R_{u\theta}$ increases up to a maximum value of 0.56 reached at $x/D_j = 5.5$, slightly downstream of the section where S_u and F_u get their extremal values ($x/D_j = 5$). Molecular effects may also be invoked here since $Pr(= \nu/\alpha)$ is equal to 0.7, but they are probably very weak since they would tend to smooth out temperature gradients more efficiently than velocity gradients, which is opposite to the present main observations.

Finally, further downstream, although S_u and F_u tend to the characteristic values of a gaussian distribution, S_θ remains slightly negative, around -0.5, and F_θ converges to a 3.3 value.

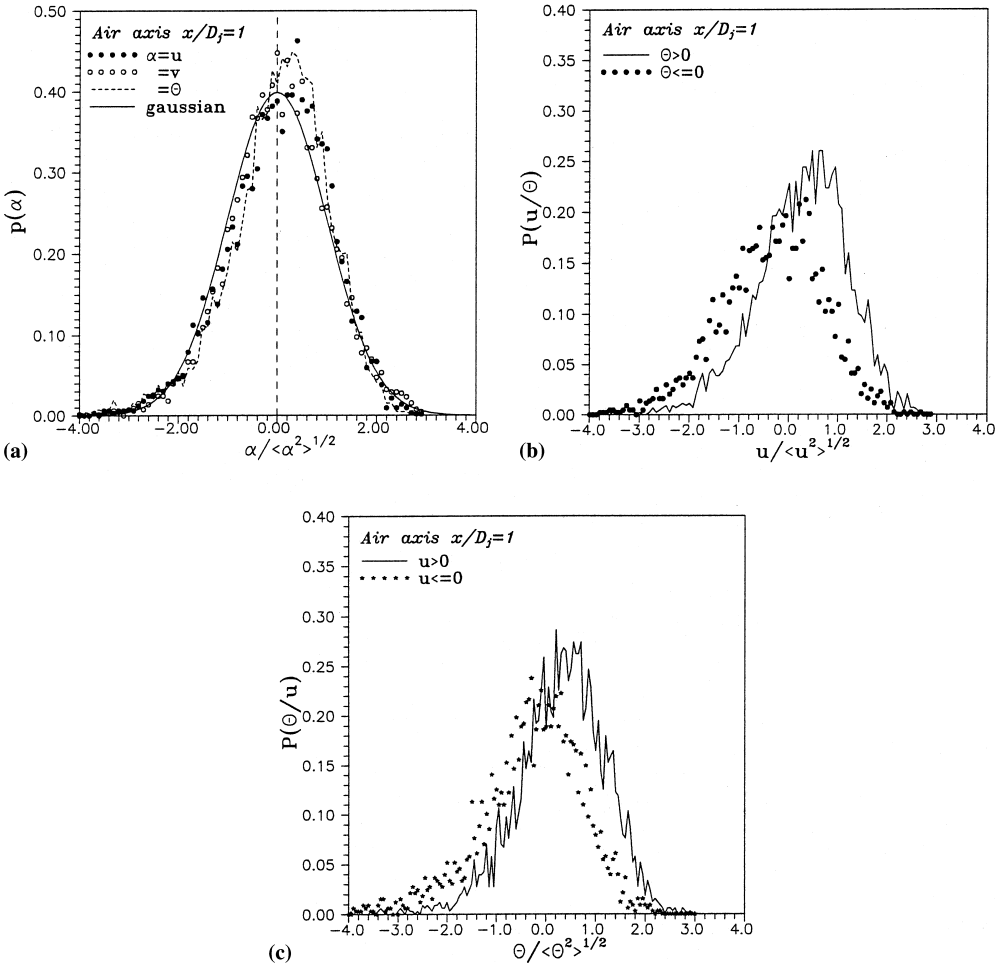

Fig. 7. P.d.f.s (a) of u, v and θ, on the axis, at the jet exit ($x/D_j = 1$), with associated conditional p.d.f.s of u (b) and θ (c).

Therefore, a slight divergence from the gaussian distribution persists for temperature in the downstream sections.

4.2. Probability density functions in the near-field region

The p.d.f.s of temperature and of the longitudinal and radial velocity components obtained on the jet axis in the near-field region are reported in Figs. 7 (at $x/D_j = 1$), 8 ($x/D_j = 3$), 9 ($x/D_j = 5$) and 10 ($x/D_j = 6$ and 6.5). Generally speaking, the velocity marginal p.d.f.s only slightly depart from an almost symmetric and almost gaussian shape. Obviously, as they are constrained by the symmetry requirements, the radial velocity p.d.f.s are those which remain closest to gaussianity, but the longitudinal velocity p.d.f.s do not differ much from the gaussian shape even at $x/D_j = 5$ where S_u and F_u get their extremal values (of about -1 and 5 respectively). On the contrary, the temperature p.d.f.s can be very different from gaussianity, with both a very marked skewed feature and a level of the maximum which can be much greater than the gaussian value of 0.4. Note that the integrals of these marginal p.d.f.s (plotted using the classical dimensionless scales) are all equal to 1. The values of T_j and T_e are mentioned in some of the figures, they are not extremal temperature values, but mean values. This explains why the presence of fluctuations slightly greater than T_j or lower than T_e may be observed on some of the graphs. In particular, it is worth mentioning that the tail of the p.d.f. corresponding to the hot temperature source T_j tends to relax very slowly since, for instance at $x/D_j = 6$ (Fig. 10a) and $x/D_j = 6.5$ (Fig. 10b), the temperature p.d.f.s reveal the coexistence of blobs of almost unmixed fluid (at temperature very close to T_j) with blobs of well-mixed fluid (associated with a gaussian like p.d.f.). The presence of blobs of "hot" fluid at temperature very close to T_j indicates that the molecular diffusivity induces very little smoothing of temperature gradients. At the opposite, the presence of blobs of "cold" fluid at rather close to ambient temperature, which appears very quickly (inducing the strong variations of S_θ and F_θ which start from x/D_j less than 1, see Fig. 6), vanishes within a few diameters.

Fig. 11, where the values (in terms of the associated r.m.s. values) of the largest positive and negative fluctuations are reported for u and θ as a function of the position x/D_j, illustrates these properties in a more precise way. The very early development of the temperature field is clearly highlighted, together with the much stronger departure from gaussian statistics for temperature than for velocity. As previously observed, the positive upper limit for temperature corresponds to the value of T_j, whereas the lower limit is never exactly equal to T_e even though negative fluctuations as strong as about $-22\ \theta'$ can be obtained. On the contrary, temperature p.d.f.s reported by Browne et al. (1984) in the interaction region of a turbulent plane jet do not show such strong negative fluctuations, but this is due, here again, to the initial conditions. For instance, by comparing the p.d.f.s reported on these authors' Fig. 12 with the $\theta'/\Delta T_j$ evolution of their Figs. 4 and 5, it is obvious that their range of temperature fluctuations exactly matches the initial temperature difference $\Delta T_j/\theta'$, whereas, as

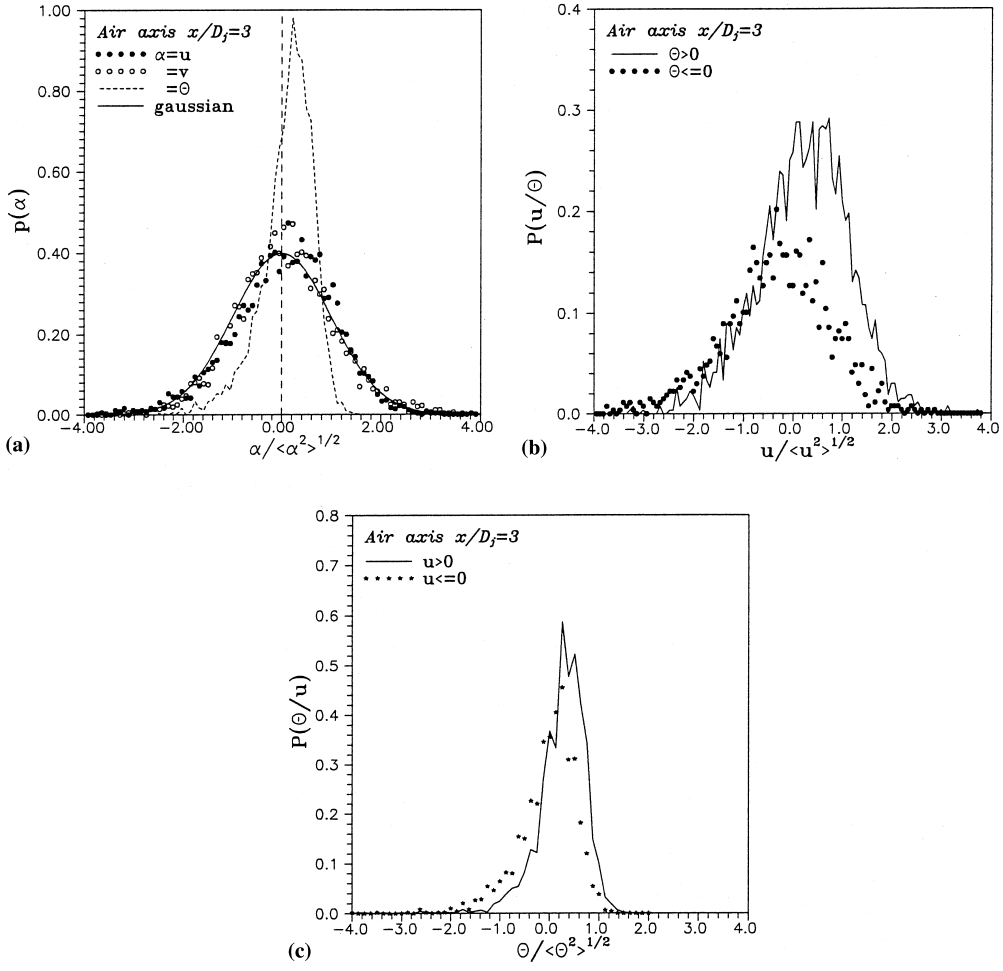

Fig. 8. P.d.f.s (a) of u, v and θ, on the axis, at the end of the thermal core ($x/D_j = 3$), with associated conditional p.d.f.s of u (b) and θ (c).

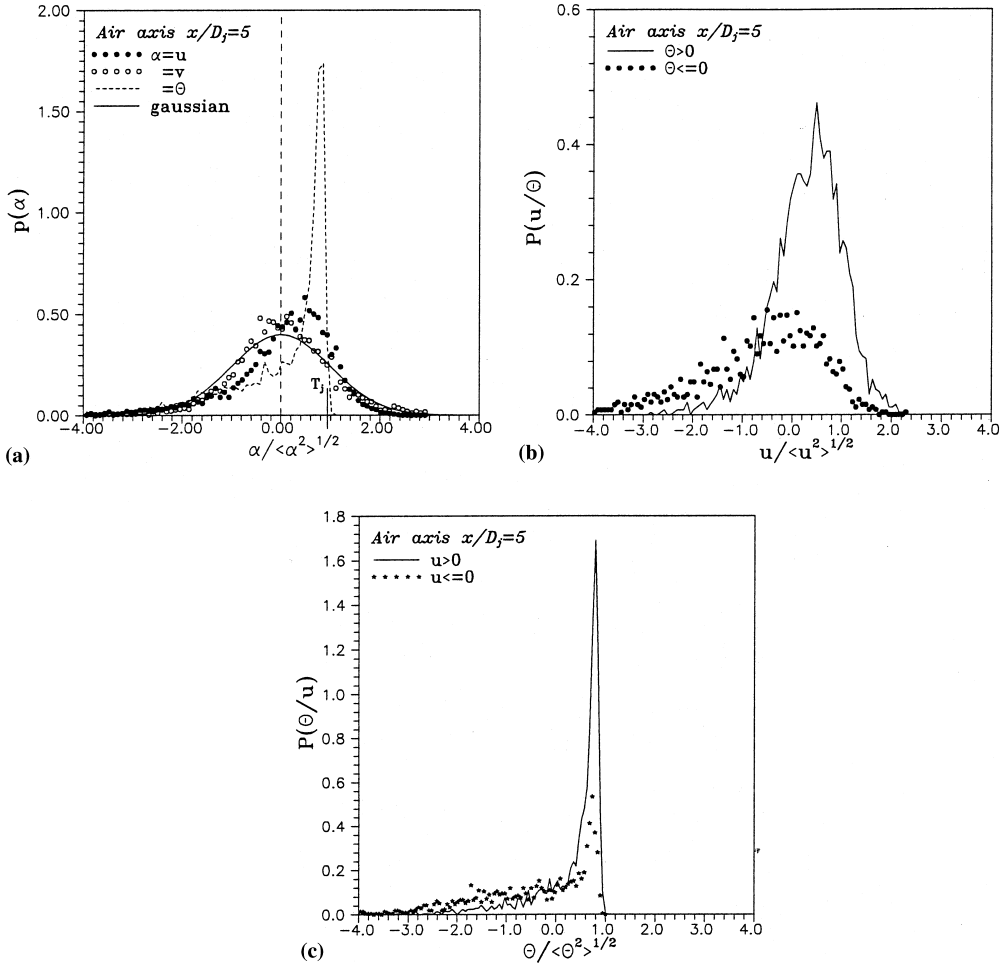

Fig. 9. P.d.f.s (a) of u, v and θ, on the axis, at the end of the potential core ($x/D_j = 5$), with associated conditional p.d.f.s of u (b) and θ (c).

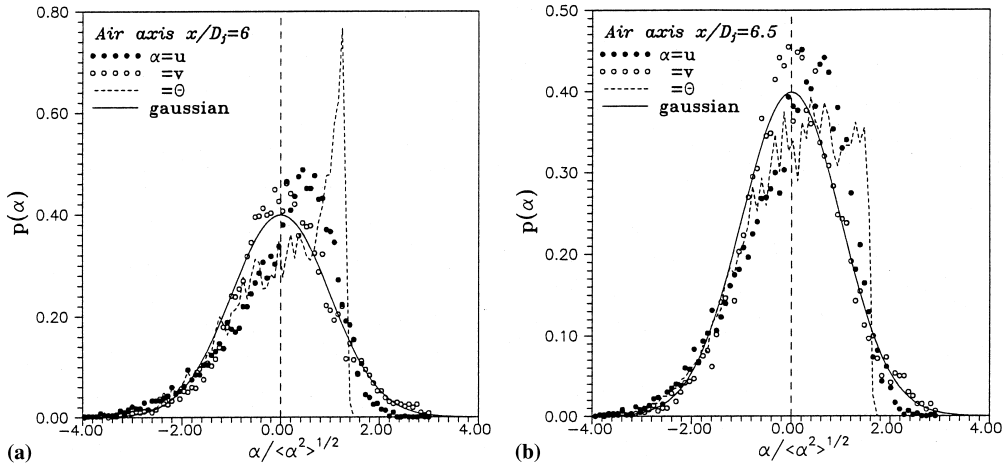

Fig. 10. P.d.f.s of u, v and θ, on the axis, at $x/D_j = 6$ (a) and at $x/D_j = 6.5$ (b).

already discussed, in our case (see Fig. 2), $\theta'/\Delta T_j$ starts from a very low level so that $\Delta T_j/\theta'$ is as large as about 140 at $x/D_j = 3$. After x/D_j about 5, the negative temperature p.d.f. tail relaxes to an almost gaussian behaviour (very similar to that for the longitudinal velocity) whereas, as observed in Figs. 9 and 10, the positive tail only relaxes after x/D_j about 7–8. Our result for the positive tail is very similar to that reported by Browne et al. (1984).

Generally speaking, the conditional p.d.f.s reflect the fact that, in agreement with the boundary constraints, in heated jets, low velocities are associated with cold temperature and large velocities with high temperature. This is particularly

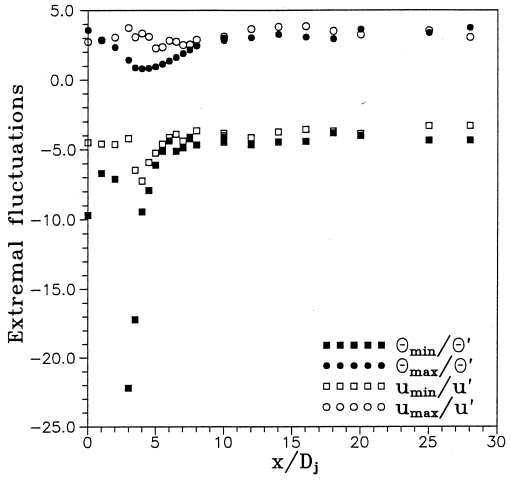

Fig. 11. Extremal normalised fluctuations of velocity and temperature on the jet axis.

obvious for the positions of the maxima of the various conditional p.d.f.s which are not located at zero (corresponding to the mean values of either temperature or velocity at the different positions), but are systematically shifted to a positive value of u (respectively θ) when conditioning is based on θ (respectively u) positive, with the inverse trend occurring when considering negative values. In addition, it is worth mentioning that these conditional p.d.f.s are not normalised with a unit area, but with an area equal to the relative number of data associated with either the positive or the negative condition. Using such a normalisation induces conditional temperature p.d.f.s (Figs. 7–9) which, for each x/D_j position, do not significantly differ for $u > 0$ and $u < 0$ as the u p.d.f.s do not deviate too much from symmetry, whereas, on the contrary, the velocity conditional p.d.f.s (Figs. 7b–9b) attain much more different levels since the occurrence of $\theta > 0$ is significantly larger than that of $\theta < 0$. On the contrary (this is not shown here due the limited space available), the extremal u fluctuations associated with the occurrence $\theta > 0$ are not very different from those associated with $\theta < 0$ (even though these extremal values satisfy the general expected property that u is more strongly negative when θ is negative and positive when θ is positive), whereas the extremal θ negative fluctuations differ noticeably for $u > 0$ and for $u < 0$, since the presence of almost unmixed ambient fluid is much more clearly detected on the θ than on the u statistical properties (see Figs. 6 and 11).

4.3. Probability density functions in the region where the jet flow is established

At the position $x/D_j = 7.5$, all second-order moments reach their maximum values before relaxing to the asymptotic stage

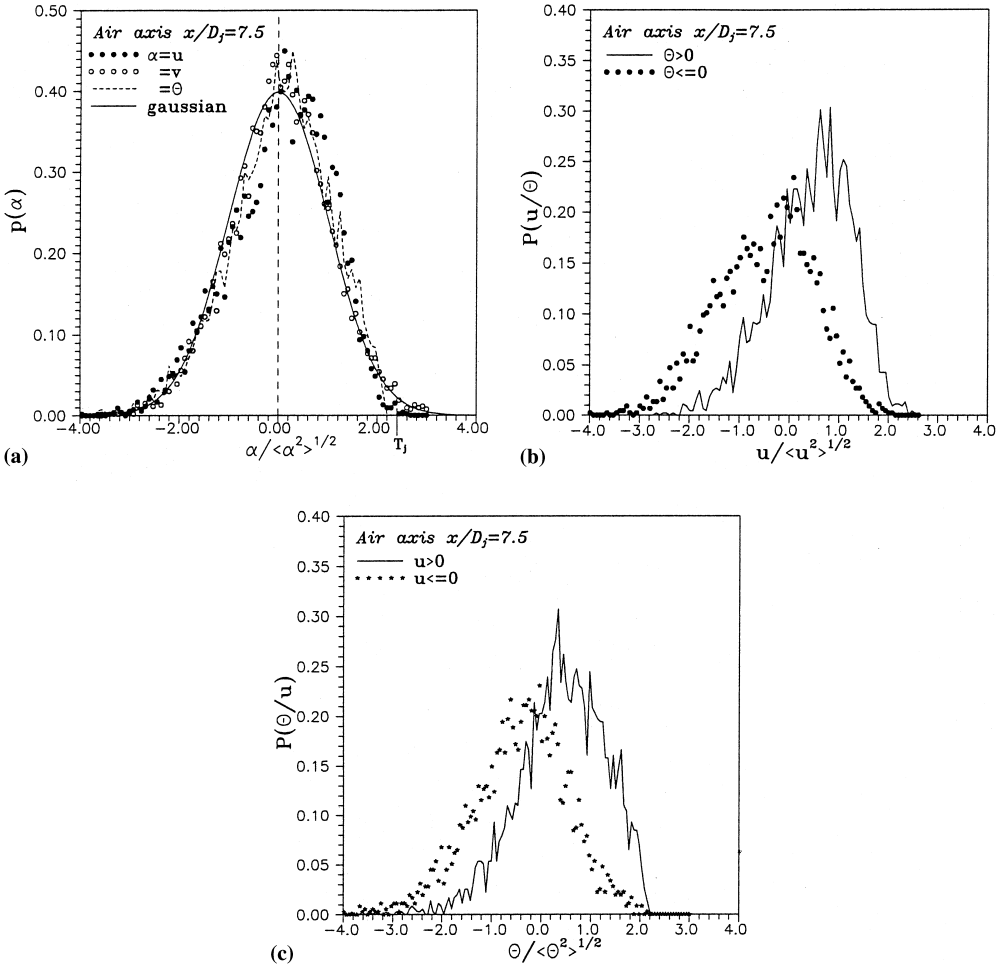

Fig. 12. P.d.f.s (a) of u, v and θ, on the axis, at $x/D_j = 7.5$, with associated conditional p.d.f.s of u (b) and θ (c).

(which begins at x/D_j about 15) where they follow power-law evolutions. Therefore, one may consider that, at this position, the jet flow is established even though self-preservation is not yet attained. The u, v and θ marginal p.d.f.s (Fig. 12) are then almost symmetric, even though the T_j hot temperature limit is still detected and slightly influencing the "hot" tail of the θ p.d.f. The u and the θ associated conditional p.d.f.s are then very similar (apart from the θ p.d.f. in the range of fluctuations next to the T_j value), as they almost reach the same levels (with about 53% of both $u > 0$ and $\theta > 0$ data, and about 47% of both $u < 0$ and $\theta < 0$ data).

Further downstream, at the section $x/D_j = 15$ (see Fig. 13), on the axis, the velocity p.d.f.s are very similar to those at $x/D_j = 7.5$, but the temperature p.d.f. skewed behaviour is then more visible than at $x/D_j = 7.5$, since the constraint imposed by T_j is relaxed but S_θ has almost the same value as at $x/D_j = 7.5$ (while F_θ is slightly increased, see Fig. 6). Therefore, the central part of the θ p.d.f. is that mainly affected by the asymmetry since rather strong negative fluctuations are maintained in the fully developed region (see Fig. 11). The conditional p.d.f.s mainly show an even better balance between the conditions of positive and negative fluctuations. In addition, Fig. 13c also shows (this property is the same at all other stations, even though such results are not reported on the previous figures) that the θ p.d.f.s conditioned by the radial velocity fluctuations v are almost perfectly identical, as is requied by the symmetry constraint.

5. Conclusion

Simultaneous measurements of two velocity components and temperature were performed in a slightly heated turbulent jet exhausting in a low velocity air coflow. A technique combining LDA and wire thermometry was optimised for this purpose. In spite of the technical problems associated with such a combination, the various results reported in this paper demonstrate the accuracy of such measurements.

Temperature acts as a passive contaminant so that it is used to mark the primary central flow without disturbing the dynamic field. The investigated region is the near-field of the jet where the velocity and temperature fields are still marked by the initial conditions, very scarce data being available. In particular, the initial profiles of velocity and temperature at the exit section are not similar so that the mean radial gradients are different. This induces a shift between the evolutions of the velocity and temperature fields (associated with a reduction of the correlation coefficient $R_{u\theta}$), as the development of the temperature field is more rapid. The turbulent Prandtl number is also affected by these different initial conditions between velocity and temperature, the result being a higher Pr_t value comparatively to results in the literature. The interface region, usually studied through the intermittency factors of velocity or temperature, was here analysed with respect to the evolution of the correlation coefficients $R_{u\theta}$, $R_{v\theta}$ and R_{uv}, and the jet edge

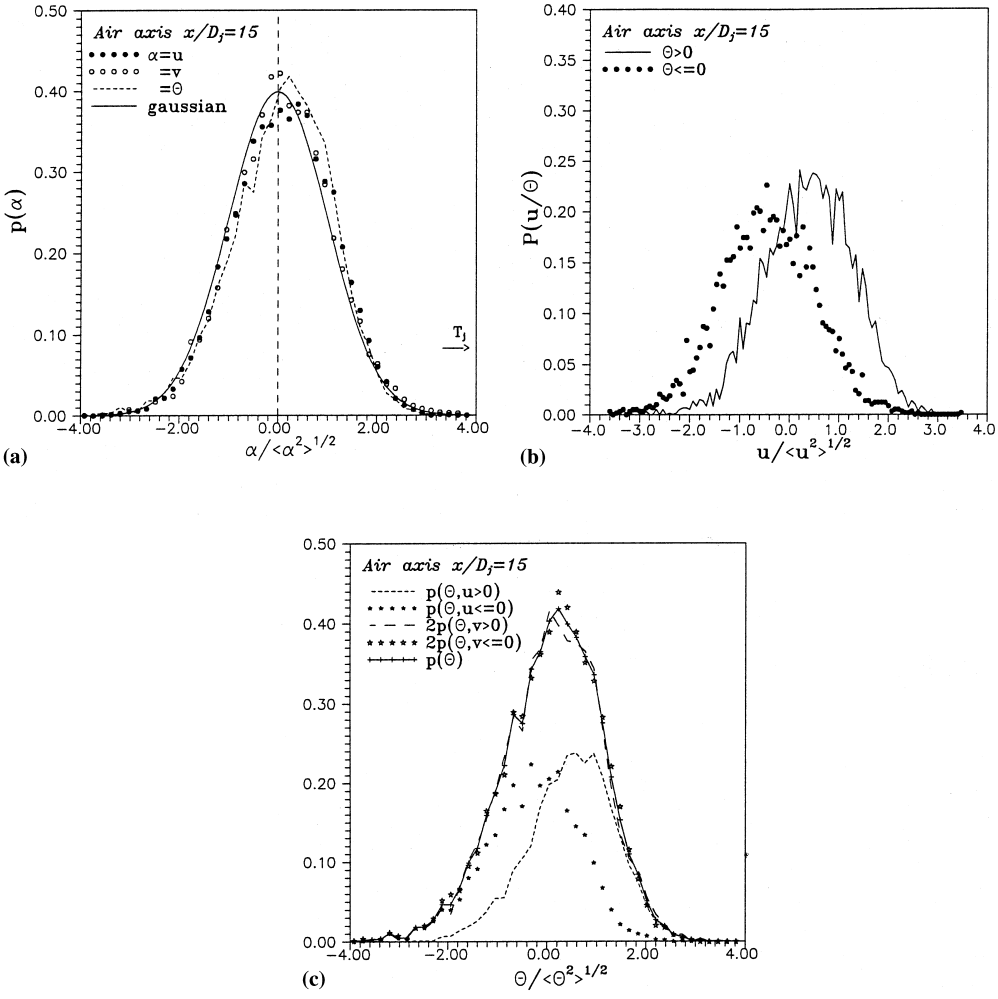

Fig. 13. P.d.f.s (a) of u, v and θ, on the axis, at $x/D_j = 15$, with associated conditional p.d.f.s of u (b) and θ (c).

was found to be characterised by a minimum of these correlation coefficients.

More detailed information about the near-field mixing properties was obtained by considering the marginal and conditional probabilities of velocity and temperature. On the axis, in the region of jet development, the influence of the "hot" limit T_j significantly constraints the temperature p.d.f. until x/D_j as large as about 7–8. Further downstream, when the jet is developed, the velocity components relax to a quasi-gaussian distribution whereas temperature remains quite far from such a distribution, with a marked negative skewness factor.

This statistical study will be complemented by the analysis of the p.d.f.s of velocity and temperature in the interface. In particular, our attention will focus on the velocities conditioned by temperature, these velocity conditional averages being both very important for better understanding the turbulence properties in the intermittent regions where the correlation coefficients $R_{u\theta}$, $R_{v\theta}$ and R_{uv} have minima and very useful for closing the p.d.f. equations in combustion models. The presently reported results suggest that the classical closure assumptions may be inadequate in these intermittent regions. More generally, the present results are a first step in our study of variable density jets and a similar procedure will be applied when the mass fraction is the scalar considered. Our final objective is the study of the turbulent mixing in flows with strong density variations.

Acknowledgements

Financial support from EDF, GDF and INERIS is gratefully acknowledged. L. Fulachier provided considerable help for the development of this research at IRPHE. We are also very grateful to S. Mucini for his contribution when working out the electronic systems.

References

Amielh, M., 1989. Etude expérimentale d'un dilueur de jet chaud. Thèse de Doctorat, Université d'Aix-Marseille II.

Anselmet, F., Djeridi, H., Fulachier, L., 1994. Joint statistics of a passive scalar and its dissipation in turbulent flows. J. Fluid Mech. 280, 173–197.

Antonia, R.A., 1985. On a heat transport model for a turbulent plane jet. Int J. Heat Mass Transfer 28 (10), 1805–1812.

Antonia, R.A., Bilger, R.W., 1976. The heated round jet in a coflowing stream. AIAA J. 14 (11), 1541–1547.

Antonia, R.A., Chambers, A.J., Hussain, A.K.M.F., 1980. Errors in simultaneous measurements of temperature and velocity in the outer part of a heated jet. Phys. Fluids 23 (5), 871–888.

Antonia, R.A., Mi, J., 1993. Temperature dissipation in a turbulent round jet. J. Fluid Mech. 250, 531–551.

Antonia, R.A., Prabhu, A., Stephenson, S.E., 1975. Conditionally sampled measurements in a heated turbulent jet. J. Fluid Mech. 72 (3), 455–480.

Bonnelye, P., 1991. Conception et réalisation d'une soufflerie pour l'étude des écoulements turbulents à masse volumique variable. Thèse C.N.A.M., I.M.S.T., Marseille.

Browne, L.W.B., Antonia, R.A., Chambers, A.J., 1984. The interaction region of a turbulent plane jet. J. Fluid Mech. 149, 355–373.

Chambers, A.J., Antonia, R.A., Fulachier, L., 1985. Turbulent Prandtl number and spectral characteristics of a turbulent mixing layer. Int. J. Heat Mass Transfer 28 (8), 1461–1468.

Chen, C.J., Rodi, W., 1980. Vertical buoyant jets – a review of experimental data. In: The Science and Appl. of Heat and Mass Transfer. Pergamon Press, New York.

Chevray, R., Tutu, N.K., 1978. Intermittency and preferential transport of heat in a round jet. J. Fluid Mech. 88 (1), 133–160.

Chua, L.P., 1989. Measurements in a turbulent circular jet. Ph.D. Thesis, University of Newcastle.

Chua, L.P., Antonia, R.A., 1990. Turbulent Prandtl number in a circular jet. Int. J. Heat Mass Transfer 33 (2), 331–339.

Djeridane, T., 1994. Contribution à l'étude expérimentale de jets turbulents axisymétriques à masse volumique variable. Thèse de Doctorat, Université d'Aix-Marseille II.

Djeridane, T., Amielh, M., Anselmet, F., Fulachier, L., 1996. Velocity turbulence properties in the near-field region of axisymmetric variable density jets. Phys. Fluids 8 (6), 1614–1630.

Fulachier, L., 1978. Hot wire measurements in low-speed heated flow. In: Proceedings of the Dynamic Flow Conference, Skovlunde, Danemark, pp. 465–485.

Gharbi, A., Amielh, M., Anselmet, F., 1995. Experimental investigation of turbulence properties in the interface region of variable density jets. Phys. Fluids 7 (10), 2444–2454.

Heitor, M.V., Taylor, A.M.K.P., Whitelaw, J.H., 1985. Simultaneous velocity and temperature measurements in a premixed flame. Exp. Fluids 3, 323–339.

Hilaire, B., 1992. Réalisation et mise en oeuvre d'un dispositif pour l'acquisition simultanée de signaux laser Doppler et fil froid. Rapport de D.E.A. Génie mécanique, INSA Toulouse.

Hussain, A.K.M.F., Zedan, M.F., 1978. Effects of the initial condition on the axisymmetricfree shear layer: effect of the initial fluctuation level. Phys. Fluids 21 (9), 1475–1481.

Klebanoff, P.S., 1954. Characteristics of turbulence in a boundary layer with zero pressure gradient. NACA Rep. 1247.

Lucas, J.F., Pietri, L., Amielh, M., Anselmet, F., Burluka, A., Borghi, R., 1998. Conditional velocity statistics in turbulent jets. In: Frisch, U. (Ed.), Advances in Turbulence VII, . Kluwer Academic Publishers, Dordrecht, pp. 561–564.

Neveu, F., Corbin, F., Perrin, V., Trinité, M., 1994. Simultaneous velocity and temperature measurements in turbulent flames obtained by coupling LDV and numerically compensated fine-wire thermocouple signals. In: Proceedings of the Seventh International Symposium on Application of Laser Techniques to Fluid Mechanics, Lisbon, Portugal, 2.4.1–2.4.8.

Ould-Rouis, M., 1995. Intermittence interne pour un scalaire passif en turbulence pleinement développée. Thèse de Doctorat, Université d'Aix-Marseille II.

Panchapakesan, N.R., Lumley, J.L., 1993. Turbulence measurements in axisymmetric jets of air and helium. J. Fluid Mech. 246, parts 1 & 2, 197–247.

Paranthoen, P., Petit, C., Lecordier, J.C., 1982. The effect of the thermal prong wire interaction on the response of a cold wire in gaseous flows (air, argon, helium). J. Fluid Mech. 124, 457–473.

Pietri, L., Mucini, S., Amielh, M., 1997. Mesures simultanées de vitesse et de température. Dispositif expérimental. Note interne I.R.P.H.E 01/97.

Pitts, W.M., 1991. Reynolds number effects on the mixing behavior of axisymmetric turbulent jets. Exp. Fluids 11 (2/3), 135–141.

Ruffin, E., 1994. Etude de jets turbulents à densité variable à l'aide de modèles de transport au second ordre. Thèse de Doctorat, Université d'Aix-Marseille II.

Ruffin, E., Schiestel, R., Anselmet, F., Amielh, M., Fulachier, L., 1994. Investigation of characteristic scales in variable density turbulent jets with a second-order model. Phys. Fluids 6 (8), 2785–2799.

Russ, S., Strykowski, P.J., 1993. Turbulent structure and entrainment in heated jets: the effect of initial conditions. Phys. Fluids 5 (12), 3216–3225.

Sautet, J.C., Stepowski, D., 1995. Dynamic behavior of variable density turbulent jets in their near development fields. Phys. Fluids 7 (11), 2796–2806.

So, R.M.C., Zhu, J.Y., Otügen, M.V., Hwang, B.C., 1991. Behavior of probability density functions in a binary gas jet. Exp. Fluids 11 (4), 227–242.

Thole, K.A., Bogard, D.G., 1994. Simultaneous temperature and velocity measurements. Meas. Sci. Technol. 5, 435–439.

Venkataramani, K.S., Tutu, N.K., Chevray, R., 1975. Probability distributions in a round heated jet. Phys. Fluids 18 (11), 1413–1420.

Wyngaard, J., 1971. Spatial resolution of a resistance wire temperature sensor. Phys. Fluids 14 (9), 2052–2054.

Zhu, J.Y., So, R.M.C., Otügen, M.V., 1988. Turbulent mass flux measurements using a laser/hot wire technique. J. Heat Mass Transfer 31, 819–829.